

Rotational isomeric state study of molecular dimensions and elasticity of perfluoropolyethers: Differences between Demnum-, Fomblin-, and Krytox-type main chains

Tomoyuki Hamada

Advanced Research Laboratory, Hitachi, Ltd, 1-280 Higashi-Koigakubo, Kokubunji-shi, Tokyo, 185-8601, Japan

Received 13th September 1999, Accepted 8th November 1999

Molecular dimensions and elasticity of Demnum-, Fomblin-Z-, and Krytox-type perfluoropolyether (PFPE) molecules were studied by rotational isomeric state (RIS) and RIS Monte Carlo (MC) methods. The mean square of end–end distance, $\langle R^2 \rangle$, that of the radius of gyration, $\langle R_g^2 \rangle$, and the characteristic ratio C_n of the molecules were calculated by the RIS method. In the RIS calculations, the number of main chain atoms, N , was increased to about 100. The RIS results show that the Demnum- and Fomblin-Z-type molecules have similar $\langle R^2 \rangle$, $\langle R_g^2 \rangle$ and C_n values. However, the Krytox-type molecule has correspondingly smaller values at every N . The molecular elasticity of the molecules was evaluated by the RIS-MC method by estimating the force–elongation relation of the molecules. These RIS-MC calculations clarified that the Demnum- and Fomblin-Z-type molecules have similar molecular elasticity, but the Krytox-type molecule is more elastic. These distinct features of the Krytox-type molecule are attributed to the distorted rotational potential of its $\text{CF}(\text{CF}_3)\text{--O}$ bonds. These calculations were compared with experimental results obtained with a surface force apparatus (SFA), and it is concluded that the Krytox-type molecule is the most desirable for boundary lubrication.

Introduction

For over three decades, perfluoropolyether (PFPE) liquids have been widely used as high-performance lubricants for aerospace and industrial uses because of their excellent tribological properties and desirable physico-chemical features such as low vapor pressure, wide liquid-temperature range, and chemical inertness. PFPE molecules are polymeric chain molecules having $\text{CF}_2\text{--O}$ bonds in their main chains and, to date, several types are commercially available; for example, Demnum[®] from Daikin Industries, Krytox[®] from E. I du Pont de Nemours & Co., and the Fomblin[®] series from Montedison Co.¹ Although PFPEs were originally developed for jet-engine lubrication systems,² nowadays, they are widely used as lubricants for magnetic hard-disks in computers because they greatly reduce adhesion between the disks and magnetic head surfaces.³ Recently, in order to achieve a higher recording density, the trend has been to reduce the gap between the disk and the head surface. As a consequence, the lubrication mode between the surfaces is changed from the conventional hydrodynamic lubrication to boundary lubrication, which can be understood only by considering the molecular behavior of lubricants under shear.

To date, several molecular orbital (MO) studies of PFPE oligomers have been reported. These studies examined molecular structures,^{1,4,5} torsion potentials,^{6–8} and degradation and tribochemical reactions of these oligomers.^{9,10} Although such MO studies provide valuable information regarding structures and chemical properties of PFPE molecules, they do not explain polymeric properties, such as viscosity, of the molecules, where these properties are directly related to lubrication. Since polymeric properties are subjects of statistical mechanics, as pointed out by Flory,¹¹ they cannot be understood by considering each molecular structure (conformation) of the molecules separately but, rather, by considering the statistical ensemble of their thermally accessible conformations.

For example, surface force apparatus (SFA) experiments by Israelachivili's group^{12,13} and Horn *et al.*¹⁴ showed that the hydrodynamic boundary thickness of polymeric boundary lubrications is determined by the radius of gyration of the polymers, R_g , which indicates the statistical average size of the polymers. These experimental studies clarified that the thickness is commensurate with R_g , both for polymer melts and solutions. Further, they found that polymeric boundary lubrications can be understood by considering a simple hydrodynamic model. This model has a hard layer of immobilized polymers on solid surfaces, and it assumes that the viscosity of polymeric liquids is equal to their bulk values outside the layer. Interestingly, this simple model appears to accord with results of an atomistic Monte Carlo (MC) simulation of a glassy-polymer/graphite interface.¹⁵ That is, the simulation investigated a hard interfacial region of one R_g thick at the polymer/graphite interface. These experiments and the simulation indicated that a statistical mechanics study of PFPE molecules is essential to understand boundary lubrication by PFPEs, which is now an important subject concerning magnetic disk lubricants.

In this study, a statistical mechanics study was made on three types of PFPE molecules, *i.e.* Demnum-, Fomblin-Z-, and Krytox-type molecular chains, by using the rotational isomeric state (RIS) method developed by Flory¹¹ and the RIS-MC method.¹⁶ The RIS and RIS-MC methods are based on equilibrium statistical mechanics and were used to predict the statistical average size and chain elasticity of the PFPE molecules. The mean square of the end–end distance, $\langle R^2 \rangle$, that of the radius of gyration, $\langle R_g^2 \rangle$, and the characteristic ratio C_n of the molecules were estimated by the RIS method. The RIS-MC method was used to calculate the mean end–end distance of these PFPE molecules under an external force applied at both their chain ends, and molecular force constants were estimated. These results show that the Krytox-type molecule has smaller molecular dimensions than the

Demnum- and Fomblin-Z-type molecules and that the Krytox-type main chain is stiffer than the other main chains. Differences between the Krytox-type and the other types of PFPE molecules were found to be caused by the different torsion potentials of the ether bonds in the molecular main chains.

Details of calculations

Perfluoropolyether molecules

Three types of PFPE molecules which have the main chain structures of Demnum[®], Krytox[®], and Fomblin-Z[®] were studied.

Demnum-type: $F-[CF_2CF_2CF_2O]_n-H$

Fomblin-Z-type: $F-[(CF_2CF_2O)-(CF_2O)]_m-H$

Krytox-type: $F-[CF(CF_3)CF_2O]_l-H$

Here, n , m , and l are chain length parameters for the Demnum-, Fomblin-Z- and Krytox-type molecules, respectively. Although the CF_2-OH group is chemically unstable and actual PFPEs having the hydroxy end group have the CF_2-CH_2-OH terminal group, the present study used these PFPE molecules for convenience. The Demnum- and Fomblin-Z-type molecules have no side chain, while the Krytox-type molecule has CF_3 side chains. The Fomblin-Z-type molecule used for the calculations is an alternating copolymer which consists of (CF_2CF_2O) and (CF_2O) units. Although the actual Fomblin-Z-PFPE is a random copolymer consisting of those units and the ratio of the former to the latter units is about 0.67, the present study used the Fomblin-Z-type molecule, assuming that the molecule can represent the actual Fomblin-Z molecule.

In the RIS calculations, the chain length parameters were increased until the number of main chain atoms N was about 100. In order to make comparisons with experiments, additional RIS calculations were made on two Fomblin-Z-type molecules, with $m = 83$ ($N = 415$) and $m = 92$ ($N = 460$), for which the molecular dimensions have already been experimentally reported.^{17,18} The RIS-MC calculations were done with N fixed at 120 because of the larger computational requirements of these calculations. This chain length is reasonable and is a typical average chain length of PFPE molecules in practical use. In these calculations, the force–elongation relation of the molecular chains was studied, and the molecular elasticity of the three types of molecules was evaluated as described in the following.

RIS and RIS-MC calculations

The RIS and RIS-MC methods were used to calculate the molecular dimensions and elasticity of the PFPE molecules. Theoretical details of these methods are described elsewhere.^{11,16} Briefly, these methods estimate statistical properties of a chain molecule at the molecular level, assuming that the main chain bonds of the molecule are in RISs. The difference between the RIS and RIS-MC methods is that the former calculates the conformation partition function of the molecule, while the latter generates several thermally accessible conformations of the molecule by using the MC scheme, in order to estimate the properties. These methods result in statistical properties of an unperturbed chain molecule at the theta point at which excluded volume effects disappear.¹¹ Since chain molecules in the melt or in the amorphous bulk state are usually unperturbed,^{19,20} these methods were assumed to be suitable for investigating molecular dimensions of PFPE lubricants, which are amorphous at room temperature.

$\langle R^2 \rangle$, $\langle R_g^2 \rangle$ and C_n of the PFPE molecules were calculated by the RIS method. The end–end distance R of a chain mol-

ecule is defined as the length of a vector which connects both molecular ends. When the molecule has n main chain bonds, its C_n is calculated as²¹

$$C_n = \frac{\langle R^2 \rangle}{\sum_{i=1}^n b_i^2}, \quad (1)$$

where b_i is the length of the main chain bond i . Similarly, $\langle R_g^2 \rangle$ of the molecule is calculated as²¹

$$\langle R_g^2 \rangle = \frac{1}{n+1} \sum_{i=0}^n \langle (r_i - R_{c.m.})^2 \rangle, \quad (2)$$

where r_i is the position vector of the main chain atom i and $R_{c.m.}$ is the position vector of the center of mass of the molecular main chain.

Insight II version 2.3²² and Polymer version 6.0²³ molecular modeling systems developed by Biosym Technologies were used for the RIS and RIS-MC calculations. The statistical weight matrices used for the calculations were evaluated by using the statistical weight utilities of the RIS module²³ in Polymer version 6.0. The statistical weight matrices of all types of bond pairs of the molecular main chains were calculated by a molecular mechanics method. Molecular mechanics calculations were made by using Discover version 2.9.5 program²⁴ and the constant valence force field (CVFF).²⁵ Here, a bond pair is defined as a molecular fragment of the PFPE molecules, which consists of a sequence of five main chain atoms and side groups attached to them.¹⁶ The statistical weight matrix of a bond pair is a quantity which contains Boltzmann factors for RISs of the pair.^{11,21} Pentane effects¹¹ were included in the RIS and RIS-MC calculations, by calculating the statistical weight matrices of such bond pairs.

The conformation energy map of a bond pair was calculated by the CVFF molecular mechanics method using the Discover program and the RIS module. Each torsion angle of the bond pair was stepped from -180 to 180° and the CVFF energy potential of the bond pair was calculated as a function of the torsion angles of the bond pair. The step size for each torsion angle was set at 12° .

The RISs of the pair were determined by fixing the energy minima of the calculated conformation energy surfaces and by combining the energy minima which are in close proximity to each other. In the present study, the tolerance of the combination was set at 20° ; that is, energy minima were combined into one if the torsion angle differences of the minima were less than 20° . All the statistical weight matrices were evaluated at 300 K.

The RIS-MC calculations generated 10^5 molecular conformations of the PFPE molecules at 300 K. The probability distribution function of the end–end distance, $p(R)$, and that of the radius of gyration, $p(R_g)$, were calculated. A single-chain force–elongation relation $r(f)$ of the molecules was calculated. The force–elongation relation $r(f)$ is the mean end–end distance of a chain molecule which is subjected to an external force f applied at both molecular ends. The force–elongation relation was estimated from the magnitude of the external force f and $p(R)$ as¹⁶

$$r(f) = \frac{\int_0^\infty dR \int_0^\pi R d\theta \cos \theta p(R) e^{fR \cos \theta / kT} R^2 \sin \theta}{\int_0^\infty dR \int_0^\pi d\theta \cos \theta p(R) e^{fR \cos \theta / kT} R^2 \sin \theta}, \quad (3)$$

where k is the Boltzmann constant, T is temperature; and θ denotes the angle between the f vector and the end–end vector of the molecule. In the present study, f was increased from zero to about $840 \text{ kJ mol}^{-1} \text{ nm}^{-1}$. Force constants k_f of the molecular chains were calculated from f and $r(f)$ as

$$k_f = f/r(f). \quad (4)$$

Results and discussion

Conformation energy and statistical weight of bond pairs

Table 1 lists bond lengths and bond angles used for the RIS and RIS-MC calculations. These values are average bond lengths and bond angles in the CVFF energy-minimum structure of the PFPE molecules with $N = 60$; that is, the shortest chain length available for all the types of the molecules. All the types of the PFPE molecules have almost the same C–C and C–O bond lengths, while some average bond angles of the molecules differ depending on the molecular types. For example, the C–O–C bond angle is 119° in the Fomblin-Z-type molecule and 124° in the Krytox-type, while the bond angle of C–C–O is almost the same in all molecular types.

Fig. 1(a)–(f) are the conformation energy maps calculated for some bond pairs of the Demnum-, Fomblin-Z-, and Krytox-type PFPE molecules. Two kinds of conformation energy maps are shown for each molecular type; that is, the maps regarding rotation of the C–C bond [Fig. 1(a), (c) and (e)] and those regarding rotation of the C–O bond [Fig. 1(b), (d), and (f)]. In Fig. 1, the energy minima are also shown by \times . They are the RISs of the bond pairs.

Fig. 1(a) and (b) are the conformation energy maps of the O–CF₂–CF₂–CF₂–O and CF₂–CF₂–O–CF₂–CF₂ bond pairs of the Demnum-type molecule, respectively. Fig. 1(a) indicates that the RISs of the O–CF₂–CF₂–CF₂–O bond pair are located in deep energy potential wells. From Fig. 1(a), the energy barriers to rotation of the CF₂–CF₂ bonds were estimated to be about 25 kJ mol^{-1} . Thus, the rotation of the CF₂–CF₂ bonds appears to be thermally restricted at room temperature. On the other hand, the potential wells around the RISs of the CF₂–CF₂–O–CF₂–CF₂ bond pair are shallower [Fig. 1(b)]. The energy barriers to rotation of the CF₂–O bonds were estimated to be less than 6.3 kJ mol^{-1} . That is, the RISs of the pair are less confined within the potential wells around them, and the bonds appear to rotate freely at room temperature. These results indicate that the CF₂–O–CF₂ moieties of the Demnum-type molecule are thermally more flexible than their CF₂–CF₂–CF₂ moieties, and the respective moieties can be regarded as soft and rigid parts of the molecules.

Fig. 1(c) and (d) are the conformation energy maps of the O–CF₂–CF₂–O–CF₂ and O–CF₂–O–CF₂–O bond pairs of the Fomblin-Z-type molecule, respectively. The conformation energy map of the O–CF₂–CF₂–O–CF₂ bond pair has unique features due to the difference in the rotational energy barriers of the CF₂–CF₂ and CF₂–O bonds. The potential curve is asymmetric with respect to $\varphi_{\text{Ca-Cb}}$ and $\varphi_{\text{Cb-Oc}}$, which are torsion angle parameters of the CF₂–CF₂ and CF₂–O bonds of this pair, respectively. The potential curve has three valleys in which the CF₂–O bond can rotate easily, but there are significant energy barriers to rotation of the CF₂–CF₂ bond. That is, the rotational energy barriers of the CF₂–CF₂ and CF₂–O bonds were estimated to be about 25 and 8 kJ mol^{-1} , respectively. These results indicate that the CF₂–CF₂ bond

cannot rotate easily, whereas the rotation of the CF₂–O bond is less thermally restricted at room temperature. The O–CF₂–O–CF₂–O bond pair of the Fomblin-Z-type molecule has lower energy barriers to rotation of the CF₂–O and O–CF₂ bonds than the CF₂–CF₂–O–CF₂–CF₂ bond pair of the Demnum-type molecule [see Fig. 1(b) and (d)]. From Fig. 1(d), the CF₂–O and O–CF₂ bonds of the Fomblin-Z-type molecule were estimated to have rotational energy barriers of less than $4\text{--}6 \text{ kJ mol}^{-1}$. Thus, CF₂–O–CF₂ moieties of the Fomblin-Z-type molecule are assumed to be thermally more flexible than those of the Demnum-type molecule.

Fig. 1(e) and (f) are the conformation energy maps of the CF(CF₃)–O–CF₂–CF(CF₃)–O and CF₂–CF(CF₃)–O–CF₂–CF(CF₃) bond pairs of the Krytox-type molecule, respectively. The energy potential curve of the CF(CF₃)–O–CF₂–CF(CF₃)–O bond pair has three valleys in which the O–CF₂ bond can rotate. This is similar to the situation for the O–CF₂–CF₂–O–CF₂ bond pair of the Fomblin-Z-type molecule. The O–CF₂ and CF₂–CF(CF₃) bonds have rotational energy barriers of about 13 and 33 kJ mol^{-1} , respectively, estimated from Fig. 1(e). Hence, the rotation of the CF₂–CF(CF₃) bond is substantially restricted at room temperature, but the rotation of the O–CF₂ bond is less restricted because of its smaller rotational energy barrier. The conformation energy map of the CF₂–CF(CF₃)–O–CF₂–CF(CF₃) bond pair [Fig. 1(f)] differs considerably from the energy maps of the corresponding bond pairs of the Demnum- and Fomblin-Z-type molecules [Fig. 1(b) and (d)]. These latter two energy potentials are very flat regarding the rotation of the O–CF₂ bonds, while the former energy potentials have significant energy barriers to rotation of the CF(CF₃)–O bond (*ca.* 17 kJ mol^{-1}). These high energy barriers can be attributed to the CF₃ side chain. These results indicate that the CF₂–CF(CF₃) and CF(CF₃)–O moieties of the Krytox-type molecule are rigid at room temperature and that only the O–CF₂ moieties provide flexibility for the Krytox-type molecule. Thus, the Krytox-type molecule is assumed to be thermally less flexible than the other types of PFPE molecules. Fig. 1(e) accords with the *ab initio* MO studies by Stanton *et al.*^{6,8} and Stanton and Schwartz.⁷ These studies showed that the CF(CF₃)–O bonds in PFPE oligomers have higher rotational energy barriers to rotation than the CF₂–O bond.

The statistical weight matrices used for the RIS and RIS-MC calculations were estimated for all types of bond pairs in the PFPE molecules and are presented in Table 2 along with torsion angles φ of the RISs of the bond pairs. The matrix elements u_{jk} of each bond pair were calculated in the form

$$u_{jk} = A_{jk} \exp(-\varepsilon_{jk}/kT), \quad (5)$$

where j and k are indices representing RISs of the first and second bonds of the bond pair, A_{jk} is a prefactor which pertains to the shape of the potential well around the rotational isomeric state jk , and ε_{jk} is the relative energy of this state with respect to the most stable RIS of the bond pair. In Table 2, b and a bonds denote the first and second bonds of the bond pairs, respectively. t means *trans* RIS, and g^- and g^+ mean *gauche*⁻ and *gauche*⁺ RISs, respectively.

Table 1 Bond lengths and angles used for RIS and RIS-MC calculations of several PFPE types

PFPE type	Bond length/nm	Bond angle/degree
Demnum	CF ₂ –CF ₂	0.158
	CF ₂ –O	0.144
Fomblin	CF ₂ –CF ₂	0.158
	CF ₂ –O	0.144
Krytox	CF(CF ₃)–CF ₂	0.158
	CF ₂ –O	0.144
	O–CF(CF ₃)	0.158

RIS results

Fig. 2(a) and (b) plot the calculated $\langle R^2 \rangle$ and $\langle R_g^2 \rangle$ of the PFPE molecules against the number of main chain atoms N , respectively. Least-squares lines are fitted to the data points. The RIS results in Fig. 2(a) and (b) show that the Demnum- and Fomblin-Z-type molecules have almost the same $\langle R^2 \rangle$ and $\langle R_g^2 \rangle$ values, whereas the Krytox-type molecule has smaller $\langle R^2 \rangle$ and $\langle R_g^2 \rangle$ values at every N . Clearly, the calculated $\langle R^2 \rangle$ and $\langle R_g^2 \rangle$ are almost proportional to N ; that is, $\langle R^2 \rangle = \alpha N + a$ and $\langle R_g^2 \rangle = \beta N + b$. Here, α , β , a and b are

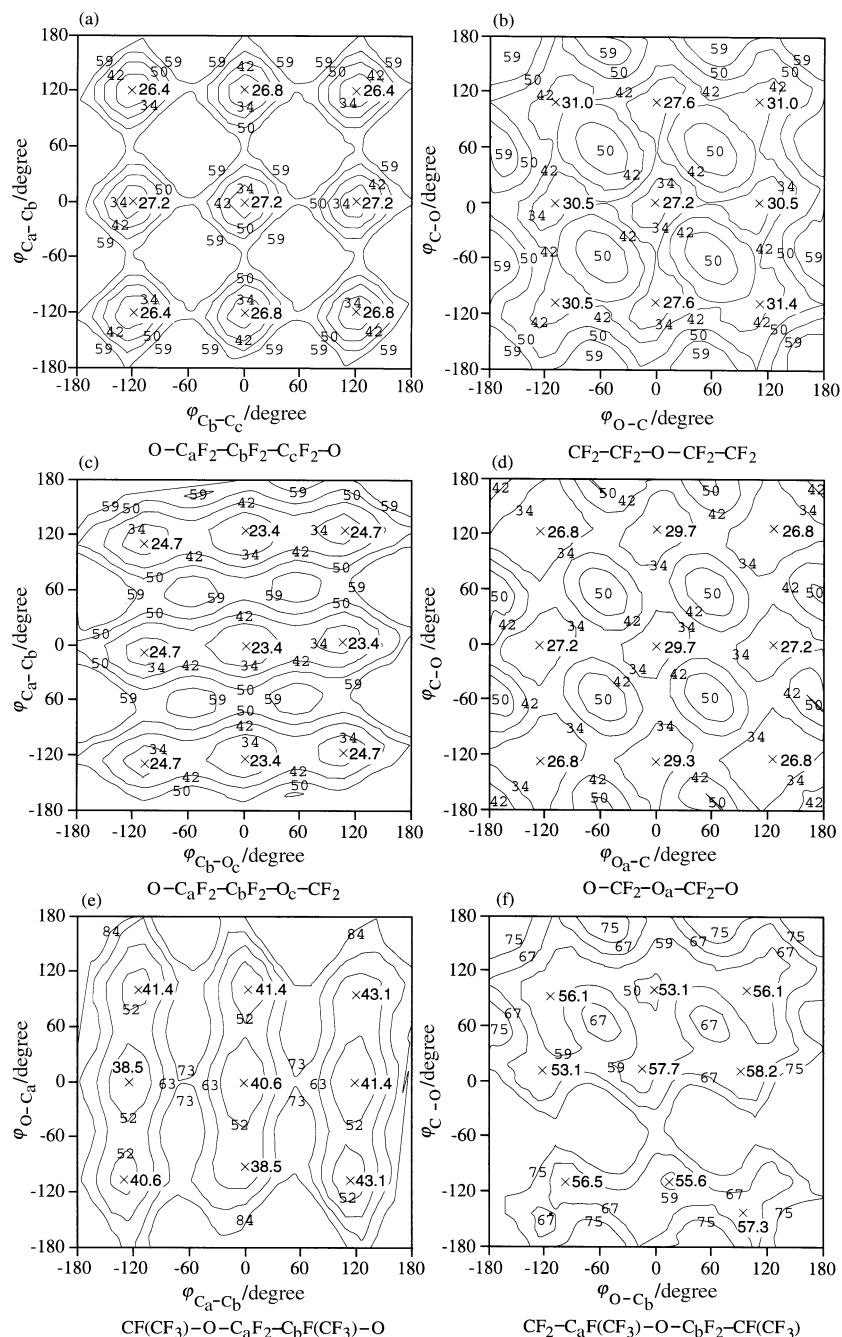


Fig. 1 Conformation energy maps of some bond pairs of Demnum-, Fomblin-Z-, and Krytox-type PFPE molecules: (a) and (b) maps of Demnum-type molecule; (c) and (d) maps of Fomblin-Z-type molecule; (e) and (f) maps of Krytox-type molecule. Energies of the contours are given in kJ mol^{-1} . The estimated energy minima are shown by \times and the CVFF energies of the minima are shown in boldface type.

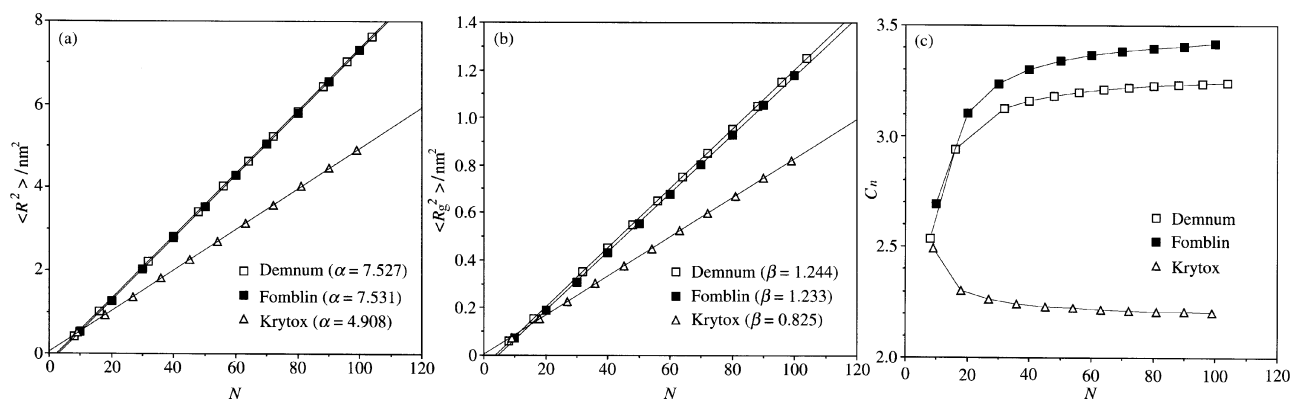


Fig. 2 Plots of (a) mean square end-end distance $\langle R^2 \rangle$, (b) radius of gyration $\langle R_g^2 \rangle$ and (c) characteristic ratio C_n of several PFPE molecules against number of atoms in main chain N .

Table 2 Calculated prefactors (dimensionless) and relative energies (kJ mol⁻¹) for statistical weight matrices of several bond pairs^a

RIS of b bond	RIS of a bond			RIS of a bond			
	<i>g</i> ⁻	<i>t</i>	<i>g</i> ⁺	<i>g</i> ⁻	<i>t</i>		
<i>g</i> ⁻	φ /degree	O-CF ₂ ^b CF ₂ ^a CF ₂ -O			CF ₂ -CF ₂ ^b CF ₂ ^a O-CF ₂		
		-121.218	0.000	121.217	-102.647	-0.249	109.904
		1.00(0.13)	0.82(0.21)	1.00(0.00)	0.65(1.38)	1.15(0.13)	0.55(1.09)
<i>t</i>		0.86(0.88)	0.82(0.84)	0.89(0.92)	0.60(1.42)	1.00(0.08)	
<i>g</i> ⁺		0.87(0.08)	0.74(0.46)	0.86(0.21)	0.57(1.09)	1.00(0.00)	
<i>g</i> ⁻	φ /degree	CF ₂ -CF ₂ ^b O ^a CF ₂ -CF ₂			CF ₂ -O ^b CF ₂ ^a CF ₂ -CF ₂		
		-105.870	-0.453	105.307	-121.244	0.000	121.244
		0.88(3.72)	0.99(0.54)	0.99(4.27)	0.88(0.25)	0.88(1.09)	0.81(1.05)
<i>t</i>		0.98(3.39)	1.00(0.00)	0.98(3.39)	1.33(0.13)	1.15(0.04)	
<i>g</i> ⁺		0.85(3.43)	0.99(0.54)	0.88(3.72)	0.98(0.63)	0.97(0.67)	
<i>g</i> ⁻	φ /degree	CF ₂ -CF ₂ ^b O ^a CF ₂ -O			CF ₂ -O ^b CF ₂ ^a O-CF ₂		
		-127.018	0.000	125.961	-121.506	-0.290	121.219
		0.99(0.46)	0.91(3.31)	0.91(0.17)	1.61(0.79)	2.00(3.39)	0.74(0.46)
<i>t</i>		1.00(0.00)	1.04(2.47)	0.99(0.00)	1.84(0.63)	1.70(3.85)	
<i>g</i> ⁺		0.91(0.17)	0.91(3.31)	0.99(0.46)	1.00(0.00)	1.75(3.35)	
<i>g</i> ⁻	φ /degree	O-CF ₂ ^b O ^a CF ₂ -O			CF ₂ -O ^b CF ₂ ^a CF ₂ -O		
		-126.252	-0.523	125.429	-120.666	-0.001	120.664
		0.87(0.33)	0.92(2.93)	1.00(0.00)	0.78(0.63)	0.82(0.96)	0.94(0.96)
<i>t</i>		0.89(0.67)	0.92(3.14)	0.87(0.71)	1.10(0.33)	1.00(0.00)	
<i>g</i> ⁺		0.93(0.42)	0.85(3.39)	0.87(0.33)	1.02(0.71)	0.88(0.54)	
<i>g</i> ⁻	φ /degree	O-CF ₂ ^b CF ₂ ^a O-CF ₂			CF ₂ -CF(CF ₃) ^b O ^a CF ₂ -CF(CF ₃)		
		-104.212	-0.251	102.786	-111.735	-3.628	100.534
		0.69(1.26)	1.16(0.13)	0.66(1.17)	0.65(3.64)	0.51(1.55)	0.71(4.27)
<i>t</i>		0.61(1.30)	1.00(0.04)	0.60(1.63)	0.00(0.00)	1.04(4.77)	
<i>g</i> ⁺		0.65(1.13)	1.00(0.00)	0.60(1.21)	0.91(2.89)	1.00(0.00)	
<i>g</i> ⁻	φ /degree	CF(CF ₃) ^b O ^a CF ₂ ^a CF(CF ₃) ^b -O			O-CF ₂ ^b CF(CF ₃) ^a O-CF ₂		
		-111.735	-3.628	100.534	-114.074	25.425	100.148
		0.67(4.51)	0.42(2.34)	0.60(4.98)	1.02(4.06)	1.87(5.31)	1.13(0.33)
<i>t</i>		0.00(0.00)	0.77(2.00)	0.48(2.97)	0.99(4.10)	1.88(5.19)	
<i>g</i> ⁺		0.88(2.00)	1.00(0.00)	0.85(2.89)	1.07(4.27)	1.89(5.15)	

^a Bond rotation angles φ of rotational isomeric states (RISs) are also shown. Relative energies are parenthesized.

the least-squares fitting parameters. As shown in the Fig. 2(a) and (b) the α and β values differ depending on the molecular types. For the Demnum- and Fomblin-Z-type molecules, these values are almost the same, while they differ substantially for the Krytox-type molecule. The RIS results show that the RIS chain is rather similar to the Gaussian chain model of a polymer with no excluded volume effects. In this model, $\langle R^2 \rangle$ and $\langle R_g^2 \rangle$ are proportional to N .²⁶ Thus, it may be worthwhile to analyze the RIS results in terms of a Gaussian chain. In the Gaussian chain model, the relation $\langle R^2 \rangle / 6 = \langle R_g^2 \rangle$ holds and, thus, β is equal to $\alpha / 6$.²⁶ This relation was used to estimate β of the three types of molecules from their α values obtained by the RIS calculations [shown in Fig. 2(a)]. The estimated β value of the Demnum- and Fomblin-Z-type molecules is 1.255 and that of the Krytox type molecule is 0.818. These estimated β values are comparable to β values calculated from the plots of $\langle R_g^2 \rangle$ [Fig. 2(b)]. These findings clearly indicate that excluded volume effects are not included in the RIS theory, although Flory¹¹ claimed that the effects can be effectively included in the theory by taking into account the pentane effects in the statistical weight calculation.

Fig. 2(c) plots the calculated C_n of the PFPE molecules against N . In all molecules, C_n tends to saturate at larger N . As for the Demnum- and Fomblin-Z-type molecules, C_n monotonously increases, while C_n of the Krytox-type molecule decreases, as N becomes larger. In the N region where C_n saturates, the Demnum-type molecule has the largest C_n and the Krytox-type molecule has the smallest C_n among the PFPE molecules studied. The Fomblin-Z-type molecule has an intermediate C_n between those of the Demnum- and Krytox-type molecules. C_n is approximately defined by

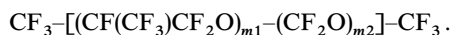
$$C_n = \frac{\langle R^2 \rangle}{nl^2} \quad (6)$$

where n is the number of main chain bonds and \bar{l}^2 is the mean square bond length.¹¹ n is equal to $N - 1$. Thus, the smallest C_n of the Krytox-type molecule accords with the fact that this molecule has the smallest $\langle R^2 \rangle$ among the PFPE molecules [Fig. 2(a)].

The differences in $\langle R^2 \rangle$, $\langle R_g^2 \rangle$, and C_n values of the PFPE molecules can be understood by considering the conformation energy potentials of the bond pairs of the molecules (Fig. 1). As can be seen in Fig. 1(e) and (f), the bond pairs of the Krytox-type molecule are energetically more stable when one bond of the bond pair is in a *gauche* state. Since *gauche* states generally have a bent main chain, preference for *gauche* states will decrease $\langle R^2 \rangle$, $\langle R_g^2 \rangle$, and consequently C_n of the molecule. Hence, the smaller $\langle R^2 \rangle$, $\langle R_g^2 \rangle$, and C_n of the Krytox type molecule can be understood in terms of this preference for the *gauche* state. On the other hand, such a preference is not significant in bond pairs of the Demnum-type molecule, as shown in Fig. 1(a) and (b). Rather, the ether bonds of the Demnum-type main chain are energetically stable when the bonds are in the *trans* state [Fig. 1(b)]. Since the *trans* state does not bend the main chain, preference for the *trans* state may increase $\langle R^2 \rangle$, $\langle R_g^2 \rangle$ and C_n of the Demnum type molecules. Thus, $\langle R^2 \rangle$, $\langle R_g^2 \rangle$, and C_n values of the PFPE molecule appear to be influenced according to which RIS is preferred, that is the *gauche* or *trans* state, in their main chains. The Fomblin-Z-type molecule has a smaller C_n than the Demnum-type molecule [Fig. 2(c)]. The smaller C_n of the Fomblin-Z-type molecule can also be explained by the fact that the ether bonds of this type of molecule favor the *gauche* state [Fig. 1(d)]. A similar result was previously obtained by Abe *et al.*²⁷ They made a RIS study of the poly(oxyethylene) (POE) molecule and found that a preference for *gauche* states in bond pairs of the molecule decreases the C_n of the molecule. The present results can be plausibly explained by assuming that the so-called “anomeric effect”^{28,29} and “*gauche*

effect^{30,31} exist in the PFPE molecules. These effects make *gauche* states of C–O–C–O and O–C–C–O structures energetically stable, respectively, and are known to exist in molecules made up of C, H, and O atoms. Namely, the anomeric effect explains the preference for *gauche* states in the O–CF₂–O–CF₂–O bond pair of the Fomblin-Z-type molecule [Fig. 1(d)], and the *gauche* effect explains the preference for *gauche* states in the CF(CF₃)–O–CF₂–CF(CF₃)–O bond pair of the Krytox-type molecule [Fig. 1(e)]. The anomeric effect and *gauche* effect also explain why the Demnum-type molecule does not show such a preference for *gauche* states because the molecule has neither the C–O–C–O nor O–C–C–O structure. On this assumption, we can conclude that the Krytox-type molecule shows the more significant preference for *gauche* states in its main chain, because the molecule has the *gauche* effect as well as the CF₃ side chain that disturbs the rotational energy potentials of the CF(CF₃)–O bond [Fig. 1(e)]. However, these effects in molecules made up of C, F and O atoms, such as the PFPE molecules, have not been investigated so far. A more elaborate *ab initio* MO study is needed in order to clarify whether these effects exist in such molecules or not.

In order to examine the accuracy of the RIS results, additional RIS calculations were made on three other PFPE molecules for which $\langle R^2 \rangle^{1/2}$ and $\langle R_g^2 \rangle^{1/2}$ have already been experimentally estimated.^{17,18} These studies measured $\langle R^2 \rangle^{1/2}$ and $\langle R_g^2 \rangle^{1/2}$ of a Fomblin-Y[®] molecule (average $M_w = 9.060$) and two Fomblin-Z[®] molecules, which have average M_w of 15 100 and 16 800, respectively. Fomblin-Y[®] is a random copolymer with the following structure:



Here, $m1$ is much larger than $m2$ ($m1 \gg m2$); hence, the molecular structure is very similar to that of the Krytox type-molecular structure. This structural similarity was taken into account and the Krytox-type molecule with $N = 162$ ($M_w = 9060$) was studied. Here, it was assumed that the molecule represents Fomblin-Y with the same M_w . Two Fomblin-Z-type molecules with $N = 415$ and $N = 460$, which have M_w of about 15 100 and 16 800, respectively, were studied. Table 3 lists the calculated and observed $\langle R^2 \rangle^{1/2}$ and $\langle R_g^2 \rangle^{1/2}$ of the molecules. Since the experimental studies reported either $\langle R^2 \rangle^{1/2}$ or $\langle R_g^2 \rangle^{1/2}$, the relation $\langle R^2 \rangle/6 = \langle R_g^2 \rangle$ was used to estimate values not reported. The RIS calculations reproduced fairly well the experimentally measured $\langle R^2 \rangle^{1/2}$ and $\langle R_g^2 \rangle^{1/2}$ of Fomblin-Z[®] with $M_w = 15\,100$. However, they underestimated these values of Fomblin-Z[®] with $M_w = 16\,800$ and Fomblin-Y[®] with $M_w = 9060$. $\langle R^2 \rangle^{1/2}$ and $\langle R_g^2 \rangle^{1/2}$ of Fomblin-Z[®] were underestimated by about 20%, and these values were underestimated by 26–34 and 31–39% for

Table 3 Calculated and observed $\langle R^2 \rangle^{1/2}$ and $\langle R_g^2 \rangle^{1/2}$ of several perfluoropolyethers (PFPEs)

PFPE Type	M_r	$\langle R^2 \rangle^{1/2}/\text{nm}$		$\langle R_g^2 \rangle^{1/2}/\text{nm}$	
		Calc.	Exp.	Calc.	Exp.
Fomblin Z	15 100	5.6	(5.8)	2.3	24 ^a
	16 800	5.9	7.3 ^b	2.4	(3.0)
			7.2 ^c	(3.0)	
Fomblin Y (Krytox)	9060	2.8	4.3 ^b	1.1	(1.8)
			3.8 ^c		(1.6)

^a Ref. 17 (viscosity measurement). ^b Ref. 18 (viscosity measurement).

^c Ref. 18 (GPC measurement).

Fomblin-Y[®]. Differences between the calculated and measured values can be attributed to the excluded volume effects that were not included in the RIS calculations, since these effects are known to influence $\langle R^2 \rangle$ and $\langle R_g^2 \rangle$.

RIS-MC results

The RIS-MC calculations were made on the Demnum-, Fomblin-Z-, and Krytox-type molecules with $N = 120$. Fig. 3(a) and (b), respectively, show the calculated $p(R/R_0)$ and $p(R_g/R_{g0})$ of the PFPE molecules. Fig. 3(a) shows that the $p(R/R_0)$ of all the molecules are Gaussian-like, except when R/R_0 is near zero. This Gaussian-like $p(R/R_0)$ is in accord with the Gaussian-chain-like behavior of the RIS chain, which was shown in the previous section. Fig. 3(b) shows that the $p(R_g/R_{g0})$ of the Demnum-type molecule is almost the same as that of the Fomblin-Z-type molecule, while the Krytox-type molecule has a different $p(R_g/R_{g0})$. Namely, the R_g distribution of the Krytox-type molecule is more dispersed than the distribution of the Demnum- and Fomblin-Z-type molecules. The dispersed conformation of the Krytox-type molecule is also shown by its $p(R/R_0)$ which is flatter and more dispersed than $p(R/R_0)$ of the other PFPE molecules.

Fig. 4(a) and (b), respectively, show the force–elongation relations $r(f)$ and force constants k_f calculated for the three types of PFPE molecules. As explained in the previous section, $r(f)$ is the mean end–end distance of the molecules subjected to an external force applied at both ends. k_f of the molecules was estimated from their $r(f)$ by using eqn. (4). All the molecules showed non-linear chain elasticity; that is, $r(f)$ tended to saturate and k_f steeply increased at larger $r(f)$. Since the molecules have a finite chain length and they cannot be lengthened further than the contour lengths of their main chains, these results are reasonable.

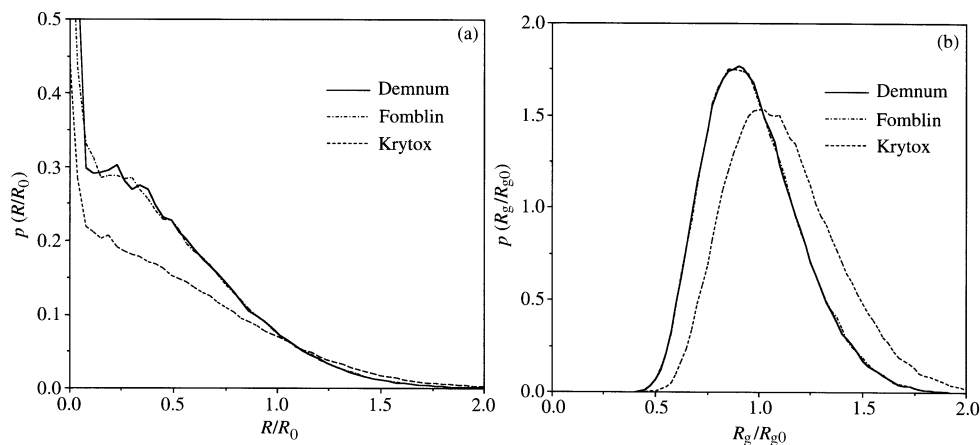


Fig. 3 RIS-MC calculations: (a) end–end distance distribution $p(R/R_0)$ and (b) radius of gyration distribution $p(R_g/R_{g0})$ of several PFPEs. R_0 and R_{g0} denote $\langle R^2 \rangle^{1/2}$ and $\langle R_{g0}^2 \rangle^{1/2}$ calculated by the RIS method, respectively.

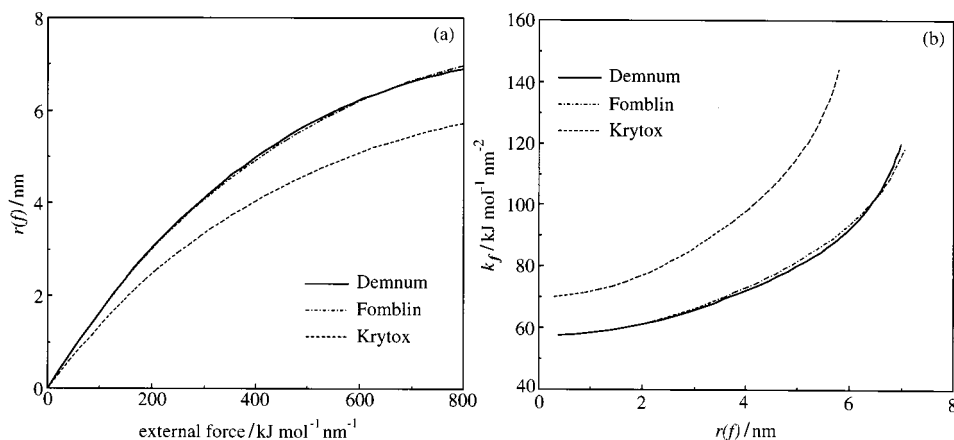


Fig. 4 Calculated molecular elasticity of several PFPE molecules: (a) force–elongation relation and (b) molecular force constant.

The above results differ from the conclusion of Kuhn's statistical theory of rubber-elasticity,³² which shows that the elasticity of a chain molecule can be attributed to the decrease of the conformation entropy of the molecule. In Kuhn's theory, k_f of a chain molecule is predicted to be constant irrespective of its elongation. Fig. 4(b) indicates that, at smaller $r(f)$, k_f of the PFPE molecules does not depend much on their elongation $r(f)$, but k_f strongly depends on $r(f)$ in intermediate and larger $r(f)$ regions. These calculations on the PFPE molecules show that the conclusion of Kuhn's theory is valid only at smaller $r(f)$. Since Kuhn's theory was originally developed for chain molecules slightly disturbed from their equilibrium structure by an external force, it is assumed to become invalid at larger $r(f)$ regions where the molecule would be significantly disturbed.

As can be seen in Fig. 4(b), the Demnum- and Fomblin-Z-type molecules have similar k_f values, but the Krytox-type molecule has a larger k_f than the other molecules. Even at smaller $r(f)$ where Kuhn's theory was thought to be appropriate [$r(f) < 1$ nm], the Krytox-type molecule has a larger k_f than the other types of molecules. These results clearly show that k_f of the PFPE molecules depends on their molecular structure. This conclusion is contrary to another conclusion from Kuhn's theory, which advocates that k_f of a chain molecule does not depend on its molecular structure. Since the main chain bonds should be forced to rotate as the molecules were lengthened, the difference in k_f of the PFPE molecules can be attributed to the rotational energy potentials of the main chain bonds. Therefore, the C–O bonds, which can rotate more easily than the C–C bonds, appear to influence $r(f)$ and k_f of the PFPE molecules. As mentioned, the rotational potentials of the CF(CF₃)–O bonds of the Krytox-type molecule are more distorted and have a higher energy barrier to rotation, because of the CF₃ side chains. The higher energy barrier to rotation may make k_f of the Krytox-type molecule larger than those of the other molecules, because a larger f is needed for rotating the CF(CF₃)–O bonds. It seems that the present results agree with the SFA experimental results of Homola *et al.*,³³ who showed that Fomblin-Y® PFPE having CF₃ side chains is more resistant to shear thinning than Fomblin-Z® with no side group.

The results of the present study indicate that the Krytox-type PFPE molecule is a suitable lubricant for boundary lubrication which causes large distortions of lubricant molecules under shear. Because of its stiffer main chain, the Krytox-type PFPE molecule seems to be more tolerant towards the larger shear stress of boundary lubrication. As mentioned above, the Krytox-type PFPE molecule has a smaller R_g than the other types of PFPE molecules. Since the hydrodynamic thickness of the polymeric boundary lubrication determines the gap between the magnetic head and disk surfaces and is approx-

imately equal to R_g ,^{12–14} this means that the gap becomes smaller when the Krytox-type PFPE molecule is used as a lubricant. On the other hand, reducing the gap is essential for a higher magnetic recording density. Thus, the Krytox-type PFPE molecule is concluded to be a favorable lubricant for a magnetic hard-disk which employs boundary lubrication in order to achieve a higher recording density, because of its smaller R_g and larger k_f .

Summary

RIS and RIS-MC calculations were made in order to estimate the molecular dimensions and elasticity of three types of PFPE molecules: Demnum®, Fomblin-Z®, and Krytox® molecules. The RIS calculations show that the Demnum- and Fomblin-Z-type molecules have similar molecular dimensions, while the molecular dimensions of the Krytox-type molecule are smaller, at all the chain lengths considered here. The RIS-MC calculations show that the main chains of the Demnum- and Fomblin-Z-type molecules have similar elasticity, while the main chain of the Krytox type molecule is more elastic. The unique features of the Krytox-type molecule are attributed to the distorted rotational energy potentials of the CF(CF₃)–O bonds. The results indicate that the Krytox-type molecule is a more desirable lubricant for the boundary lubrication of magnetic hard-disks, due to its smaller molecular size and larger molecular elasticity than the other types of PFPE.

References

- 1 P. H. Kasai, *Macromolecules*, 1992, **25**, 6791.
- 2 C. E. Snyder, Jr., L. J. Gschwendner and C. Tamborski, *Lubr. Eng.*, 1981, **27**, 344.
- 3 M. Barlow, M. Braitberg, L. Davis, V. Dunn and D. Frew, *IEEE Trans. Magn.*, 1987, **mag-23**, 33.
- 4 J. Pacansky and B. Liu, *J. Phys. Chem.*, 1985, **89**, 1883.
- 5 J. Pacansky, M. Miller, W. Hatton, B. Liu and A. Scheiner, *J. Am. Chem. Soc.*, 1991, **113**, 329.
- 6 C. L. Stanton, H. L. Paige and M. Schwartz, *J. Phys. Chem.*, 1993, **97**, 5901.
- 7 C. L. Stanton and M. Schwartz, *J. Phys. Chem.*, 1993, **97**, 11221.
- 8 C. L. Stanton, R. J. Berry and M. Schwartz, *J. Phys. Chem.*, 1995, **99**, 3473.
- 9 S. Matsunuma, T. Miura and H. Kataoka, *Tribol. Trans.*, 1996, **39**, 380.
- 10 S. Matsunuma, *Wear*, 1997, **213**, 112.
- 11 P. J. Flory, *Statistical Mechanics of Chain Molecules*, Hanser Publishers, New York, 1989.
- 12 R. G. Horn and J. N. Israelachvili, *Macromolecules*, 1988, **21**, 2836.
- 13 J. N. Israelachvili, S. J. Kott and L. J. Fetters, *J. Polym. Sci. B*, 1989, **27**, 489.
- 14 R. G. Horn, S. J. Hirz, G. Hadziioannou, C. W. Frank and J. M. Catala, *J. Chem. Phys.*, 1989, **90**, 6767.

- 15 K. F. Mansfield and D. N. Theodorou, *Macromolecules*, 1991, **24**, 4295.
- 16 *Polymer Ver. 6.0 User Guide Part 2*, Biosym Technologies, San Diego, CA, 1993, ch. 11.
- 17 J. P. Monfort and G. Hadziioannou, *J. Chem. Phys.*, 1988, **88**, 7187.
- 18 M. J. R. Cantow, R. B. Larrabee, E. M. Barrall, J. R. Butner, P. Cotts, F. Levy and T. Y. Ting, *Makromol. Chem.*, 1986, **187**, 2475.
- 19 P. J. Flory, *J. Chem. Phys.*, 1949, **17**, 303.
- 20 P.-G. de Gennes, *Scaling Concepts in Polymer Physics*, Cornell University Press, Ithaca, NY, 1979, ch. II.
- 21 J. D. Honeycutt, in *Physical Properties of Polymer Handbook*, ed. J. E. Mark, American Institute of Physics, New York, 1996, p. 39.
- 22 *Insight II Ver. 2.3.0*, Biosym Technologies, San Diego, CA, 1993.
- 23 *Polymer Ver 6.0*, Biosym Technologies, San Diego, CA, 1993.
- 24 *Discover Ver. 2.9.5*, Biosym Technologies, San Diego, CA, 1994.
- 25 *Discover Ver. 2.9.5 User Guide Part 1*, Biosym Technologies, San Diego, CA, 1994, ch 3.
- 26 M. Doi and S. F. Edward, *The Theory of Polymer Dynamics*, Clarendon Press, Oxford, 1986, ch. 2.
- 27 A. Abe, K. Tasaki and J. E. Mark, *Polym. J.*, 1985, **17**, 883.
- 28 G. A. Jeffrey, J. A. Pople and L. Radom, *Carbohydr. Res.*, 1972, **25**, 117.
- 29 A. Abe, *J. Am. Chem. Soc.*, 1976, **98**, 6477.
- 30 J. E. Mark and P. J. Flory, *J. Am. Chem. Soc.*, 1965, **87**, 1415.
- 31 K. Tasaki and A. Abe, *Polym. J.*, 1985, **17**, 641.
- 32 W. Kuhn, *Kolloid-Z.*, 1936, **76**, 258.
- 33 A. M. Homola, H. V. Nguyen and G. Hadziinannou, *J. Chem. Phys.*, 1991, **94**, 2346.

Paper a907414g